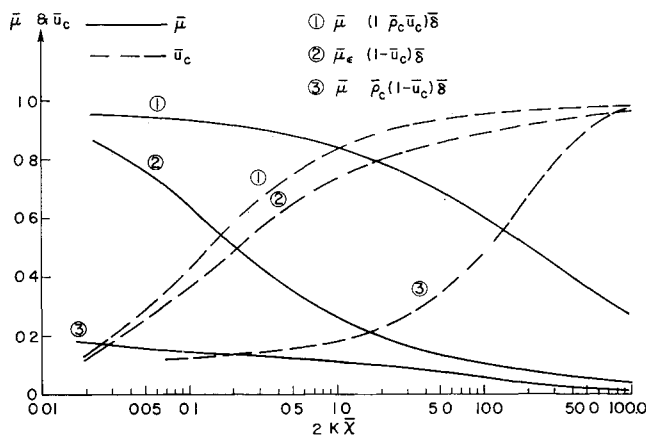


**Fig 2 Variations of axis enthalpy; slender cone, altitude = 150,000 ft,  $M_\infty = 19.52$**

for the three different forms of the eddy viscosity coefficients. For case 3, this distance is  $(2K\bar{x})\bar{h}_{cmx} = 10$ , which is two orders of magnitude higher than case 1, where  $(2K\bar{x})\bar{h}_{cmx} = 0.1$ , whereas in case 2,  $(2K\bar{x})\bar{h}_{cmx} = 0.2$ . The constant  $K$  is generally considered to be in the order of  $10^{-2}$  whereas the initial viscous wake width is in the order of the base radius of the body. Therefore, in terms of the physical distance, the off-axis peak enthalpy reaches the axis at a distance approximately equal to 500 base radii from the initial axial station for case 3, whereas it is only 10 and 5 base radii for cases 2 and 1, respectively. Since the peak enthalpy is off the axis from  $\bar{x} = 0$  up to  $\bar{x} = \bar{x}_{h_{cmx}}$ , hence the hottest portion of the wake also spreads through this region. This hottest portion of the wake is, therefore, approximately 500 base radii long for case 3, compared with 10 and 5 base radii for cases 2 and 1, respectively, for the conditions used in the present calculations. Since the external inviscid conditions are assumed uniform, the electron density distribution follows the same trend as the enthalpy distribution.

It is further noted that the variations of the centerline enthalpy for these three cases can be predicted qualitatively by the values of their corresponding eddy viscosity coefficients (Fig 3). In the present case, the centerline enthalpy is larger than the inviscid enthalpy. Therefore,  $\rho$  is smaller than  $\rho$  and hence the value of  $\mu_{e3}$  is smaller than  $\mu_{e2}$  and they are in turn smaller than  $\mu_{e1}$  [Eqs (1-3)]. With a smaller  $\mu_e$  or slower diffusion process, a slower axial change of  $a$  [Eq (10)] and hence those of  $\bar{\rho}u$ ,  $\bar{u}$ , and  $\bar{h}$  result. This is clearly indicated in Figs 2 and 3.



**Fig 3 Variations of axis velocity and eddy viscosity coefficient; slender cone, altitude = 150,000 ft,  $M_\infty = 19.52$**

The forementioned reasoning generally applies to a slender cone under hypersonic flight conditions. Therefore, the significant differences in the equilibrium turbulent-wake characteristics due to the different forms of the eddy viscosity coefficient as given here may be considered as typical for a hypersonic slender cone.

Since all the three forms of the eddy viscosity coefficients considered here reduce to the same form in incompressible case but give different results for the wake characteristics, firmer ground derived from experimental evidence on which the selection of the form of the eddy viscosity coefficient can be based is much needed.†

**References**

- <sup>1</sup> Wan, K S, "Hypersonic laminar and turbulent wakes at chemical equilibrium," General Electric Co GE MSD TIS R63SD01 (August 1963)
- <sup>2</sup> Bloom, M H and Steiger, M H, "Diffusion and chemical relaxation in free mixing," IAS Paper 63-67 (January 1963)
- <sup>3</sup> Lees, L and Hromas, L, "Turbulent diffusion in the wake of a blunt nosed at hypersonic speeds," J Aerospace Sci 29, 976-993 (1962).
- <sup>4</sup> Ting, L and Libby, P A, "Remarks on the eddy viscosity in compressible mixing flows," J Aerospace Sci 27, 797-798 (1960)
- <sup>5</sup> Li, H, "Hypersonic non equilibrium wakes of a slender body," General Electric Co GE MSD TIS R63SD50 (to be published)
- <sup>6</sup> Wan, K S, "Comparison of turbulent wake characteristics based on different eddy viscosity coefficients," General Electric Co GE MSD TIS R63SD71 (September 1963)
- <sup>7</sup> Zeiberg, S L and Bleich, G D, "Finite difference calculation of hypersonic wakes," AIAA Paper 63-448 (August 1963)
- <sup>8</sup> Ferri, A, Libby, P A, and Zakkay, V, "Theoretical and experimental investigation of supersonic combustion," Aeronaut Res Labs Rept 62-467 (September 1962)

† After this work had been completed, Ref 7 came to the author's attention. The same problem treated here is also considered in that work with a finite difference method of solution, using the exact expressions given in Refs 2-4 and 8. The conclusions agree qualitatively with the present work.

**Correlation of Boost Phase Turbulent Heating Flight Data**

MICHAEL G DUNN\*

Lockheed Missiles and Space Company, Sunnyvale, Calif

**Nomenclature**

- $c_p$  = specific heat at constant pressure
- $G$  = axisymmetric factor defined by Eq (3)
- $h$  = convective heat transfer coefficient
- $k$  = coefficient of thermal conductivity
- $Nu^*$  = Nusselt number,  $hs/k^*$
- $P$  = pressure
- $Pr^*$  = Prandtl number,  $\mu^*c_p^*/k^*$
- $r$  = radius of surface point from axis of symmetry
- $R_b$  = nose radius of curvature
- $Re_s^*$  = Reynolds number,  $\rho^*u_s/\mu^*$
- $s$  = boundary layer length
- $u$  = velocity component parallel to surface
- $\gamma$  = specific heat ratio
- $\mu$  = dynamic viscosity
- $\rho$  = density

Received September 25, 1963

\* Associate Research Scientist Member AIAA

**Subscripts**

- $e$  = evaluated at local edge of boundary-layer conditions
- $\infty$  = evaluated at freestream conditions
- $t$  = evaluated at local stagnation conditions

**Superscript**

- \* = evaluated at Eckert reference temperature

**Introduction**

THE problem of predicting turbulent boundary-layer aerodynamic heating to unyawed bodies of revolution has received considerable attention in recent years. The prediction of aerodynamic heat-transfer rates depends upon a knowledge of the detailed boundary-layer characteristics. Solutions of the boundary-layer conservation equations often can be obtained with a high degree of precision for laminar flows, whereas turbulent boundary-layer solutions are less exact and involve the use of empirical laws. The purpose of this note is to illustrate the correlation between recent flight data and two suggested methods of predicting turbulent boundary-layer aerodynamic heat transfer.

The flight data reported herein were obtained from a satellite vehicle at freestream Mach numbers ranging from 1.41–4.20, and freestream Reynolds numbers ranging from  $3.02 \times 10^6/\text{ft}$  to  $2.62 \times 10^6/\text{ft}$ . The 1959 Air Research and Development Command atmosphere was utilized throughout the calculations presented herein. Figure 1 illustrates the vehicle configuration and variation of freestream trajectory parameters. Instrumentation consisted of silicon semiconductors which were located on the cylindrical section between 5 and 27 in from the beginning of the cylindrical section as shown on Fig. 1. Preflight measurements of skin thickness (nominal 0.071 in magnesium) and pictures of the installation were obtained to aid in the data reduction. A surface emissivity of 0.75 consistent with the surface specifications was used for the calculation of the radiation heat transfer and was assumed to be constant. A postflight analysis was conducted to determine the vehicle pitch and yaw time histories. The results of this study indicated that the maximum variation of the total angle of attack in the time interval for which data are reported was less than  $\pm 0.5^\circ$ .

**Data Reduction**

The inviscid flow field was obtained from a combination of the Swigart<sup>1</sup> blunt-body solution and a method of characteristics solution proposed by Benson.<sup>2</sup> The Swigart solution,

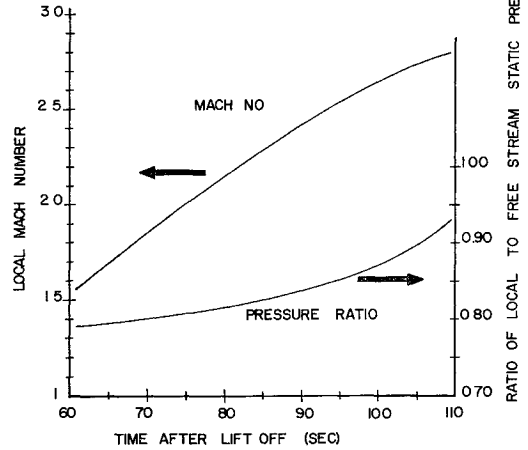
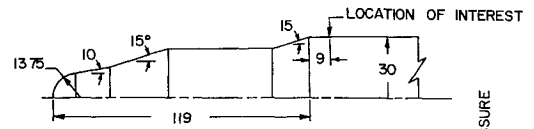


Fig 2 Variation of local flow-field parameters

which solves for the flow in the subsonic and transonic regions behind the bow shock, is used to determine the starting line for the method of characteristics solution. A detailed description of the flow-field calculation procedure is presented by Lanfranco.<sup>3</sup> Figure 2 presents the variation with time of the local Mach number and static pressure ratio for the section located between 5 and 12 in from the flare-cylinder junction.

A simple thin-skin analysis which considered both convection and external radiation was used to calculate the surface heat fluxes. The thermal model assumed that energy exchange could occur only at the external surface. During the time interval for which data are reported, internal radiation and substructure conduction were negligible and thus were neglected. In order to simplify the presentation and to average data scatter, the convective heat rates calculated for the instrumented sections (4 sensors in each location) located between 5 and 12 in and 21 and 27 in from the flare-cylinder junction were arithmetically averaged and considered to represent the convective heat rates at the midpoint of the respective section. Prior to 90 sec after lift-off, the average values of the heat rates were computed at 2-sec intervals. Between 90 and 103 sec the averages were computed at 1-sec intervals. Reduction of the data was performed on an IBM 7090 digital computer. Use was made of the averaged heat rates to calculate the corresponding heat-transfer coefficients. These heat-transfer coefficients were used for the calculation of the Nusselt numbers, which are presented in Fig. 3 as a function of local Reynolds number with properties evaluated at the Eckert<sup>4</sup> reference temperature.

**Data Correlation**

Two methods of predicting turbulent boundary-layer convective heat transfer are compared to the flight data. The first technique is that suggested by Bromberg<sup>5</sup> et al and modified by Hearne<sup>6</sup> et al for calculating convective heat transfer to a body of revolution. Application of this technique yields the following expression for the Nusselt number,

$$Nu^* = 0.0289 (Pr^*)^{0.333} (Re_s^*)^{0.5} G(s/R_b) \quad (1)$$

where

$$G(s/R_b) = \left[ \int_0^{s/R_b} \frac{(\rho_e/\rho_\infty)(u/u_\infty)(\mu_e/\mu_\infty)^{0.25}(r/R_b)^{1.25}(s/R_b)}{(\rho/\rho_\infty)(u/u_\infty)(\mu/\mu_\infty)^{0.25}(r/R_b)^{1.25}d(s/R_b)} \right]^{0.20} \quad (2)$$

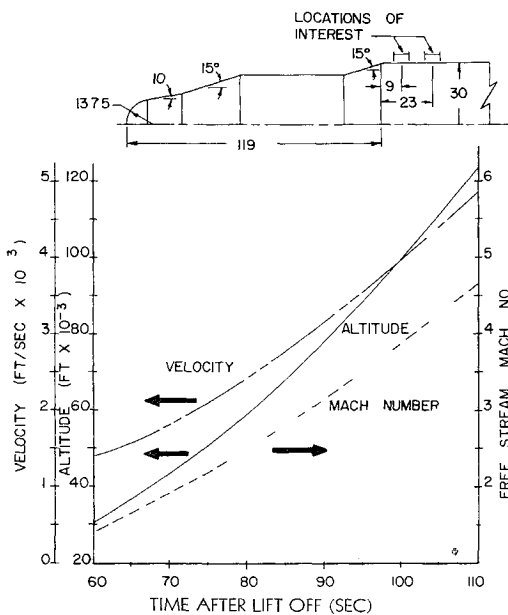


Fig 1 Freestream trajectory parameters

By successive application of isentropic flow relations along the stagnation point streamline in the region bounded by the stagnation point and the conical shock, the region bounded by the conical shock and the flare shock, and the region bounded by the flare shock and the point of interest, one can reduce Eq (2) to the following form:

$$G\left(\frac{s}{R_b}\right) = \left[ \frac{(P_e/P_t)^{(5\gamma+19)/24\gamma_e} [1 - (P_e/P_t)^{(\gamma-1)/\gamma}]^{0.5} (r/R_b)^{1.25} (s/R_b)}{\int_0^{s/R_b} (P/P_t)^{(5\gamma+19)/24\gamma_e} [1 - (P/P_t)^{(\gamma-1)/\gamma}]^{0.5} (r/R_b)^{1.25} d(s/R_b)} \right]^{0.2} \quad (3)$$

A second heat-transfer calculation technique which is often used in the literature for data correlation is that suggested by Eckert.<sup>4</sup> The corresponding Nusselt number correlation can be represented as follows:

$$Nu^* = 0.0296 (Pr^*)^{0.333} (Re_s^*)^{0.8} \quad (4)$$

The two methods just outlined were utilized to obtain the correlation between predictions and data presented in Fig 3. Initially, Eqs (1) and (4) were used to predict Nusselt numbers for each of the instrumented sections. However, the results were nearly the same; thus an average value is presented. Early time (high Reynolds number) data are subject to inaccuracies because of the small difference between the recovery and wall temperatures. At a flight time of 100 sec when the local Reynolds number is approximately  $10^6$ , boundary-layer transition appears to commence. Therefore, subsequent data cannot be compared with the turbulent predictions.

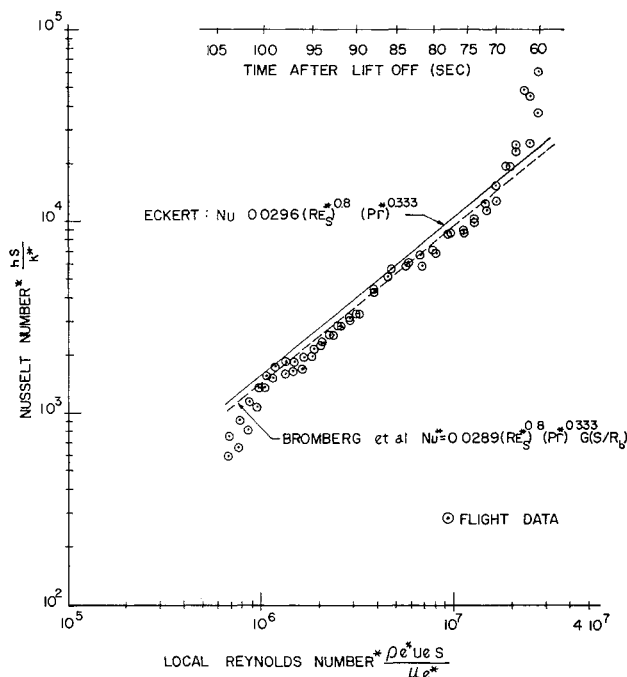


Fig 3 Comparison of observed and predicted Nusselt numbers

### Conclusions

A correlation between two turbulent boundary-layer heat-transfer prediction techniques and recent flight data has been presented. The Eckert correlation results in predicted Nusselt numbers which are approximately 10% greater than corresponding Bromberg values.

### References

- Swigart, R. J., "A theory of asymmetric hypersonic blunt-body flows," AIAA J 1, 1034-1042 (1963)
- Benson, J. L., "The method of characteristics and its application to digital computer solutions of some supersonic flow prob-

lems," Lockheed California Co, Rept 13606 (October 1959)

<sup>3</sup> Lanfranco, M. J., "A solution of the supersonic flow past blunt bodies of revolution," Lockheed Missiles and Space Co TM 5341-17, LMSC A362449 (November 1963)

<sup>4</sup> Eckert, E. R. G., "Survey of boundary layer heat transfer at high velocities and high temperatures," Wright Air Dev

Center TR 59 624 (April 1960)

<sup>5</sup> Bromberg, R., Fox, J. L., and Ackermann, W. G., "A method of predicting convective heat input to the entry body of a ballistic missile," Ramo-Woolridge Corp., Los Angeles, Calif (June 1956); confidential

<sup>6</sup> Hearne, L. F., Hines, F. L., and Rindal, R. A., "Recommended procedures for prediction of re entry convective heating environment," Lockheed Missiles and Space Co, TIAD/201 (September 1960)

## Transient Temperature Variation in a Thermally Orthotropic Cylindrical Shell

K. J. TOURYAN\*

Sandia Corporation, Albuquerque, N. Mex

An analysis is carried out to study the two-dimensional transient heat-transfer characteristics of a thin, anisotropic cylindrical shell. An arbitrary heat input is assumed on the front face of the shell and the rest of the surfaces are assumed to be insulated.

GIEDT and Hornbaker<sup>1</sup> carried out an analysis to study the time-temperature history in a thermally anisotropic plate. Such solutions have recently become necessary because of the increased use of such highly anisotropic materials as pyrolytic graphite for thermal protection.

A similar solution applied to an infinite cylindrical shell (Fig 1) will be discussed here, subject to the same boundary conditions as those given by Giedt and Hornbaker. The Fourier law of conduction for an anisotropic medium in cylindrical coordinates is given by

$$\frac{\partial v}{\partial t} = \kappa \left[ \frac{\partial^2 v_r}{\partial r^2} + \frac{1}{r} \frac{\partial v_r}{\partial r} \right] + \frac{\kappa_\theta}{r^2} \frac{\partial^2 v_\theta}{\partial \theta^2} \quad (1)$$

- $\kappa_r$  = thermal diffusivity in the  $r$  direction
- $\kappa_\theta$  = thermal diffusivity in the  $\theta$  direction
- $k_r$  = thermal conductivity in the  $r$  direction
- $v$  = temperature
- $t$  = time

Now let

$$r' = \frac{r}{(\kappa_r)^{1/2}} \quad \theta' = \theta \left( \frac{\kappa_r}{\kappa_\theta} \right)^{1/2} \quad (1a)$$

Substitution of these new variables in Eq (1) gives

$$\frac{\partial v}{\partial t} = \frac{\partial^2 v_r}{\partial r'^2} + \frac{1}{r'} \frac{\partial v_r}{\partial r'} + \frac{1}{r'^2} \frac{\partial^2 v_\theta}{\partial \theta'^2} \quad (2)$$

The appropriate initial and boundary conditions are

$$\frac{\partial v}{\partial r'} = 0 \text{ at } r' = \frac{a}{(\kappa_r)^{1/2}} = a' \quad 0 < \theta < \theta_0 \quad (2a)$$

Received September 23, 1963

\* Staff Member, Aerophysics Section